

**PROTEIN ENRICHMENT OF *PYCNOPORUS SANGUINEUS* FOR  
SILVER NANOPARTICLES SYNTHESIS**

**by**

**CHAN YEN SAN**

**Thesis submitted in fulfilment of the requirements for the degree of  
Doctor of Philosophy**

**FEBRUARY 2014**

## ACKNOWLEDGEMENT

It is with immense gratitude that I acknowledge the support and help of my supervisor, Dr Mashitah Mat Don, who has the attitude and the substance of a genius; she suggested the topic of this thesis and who miraculously supervised the execution of the experimental work and was always there with her guidance and constructive criticism. Without her guidance and persistent help this dissertation would not have been possible.

My sincere thanks are also to Professor Dr. Abdul Rahman Bin Mohamed and Dr. Lim Jit Kang who have co-supervised my work and gave their valuable guidance and discussions of this work. I am deeply grateful to Dr Lim who has been always there to listen and have long discussions that helped me sort out the technical details of my work.

I owe my deepest gratitude to my grandmother, Yoon Swee Wah who loves and always support me for whatever decisions that I have made. Without her love and support no work can be done. Also, I would like to express my heart-felt gratitude to my other family members; none of this would have been possible without the love and patience of them.

Finally, I appreciate the financial support from Research University Grant, Fundamental Research Grant Scheme, Postgraduate Research Grant Scheme and Universiti Sains Malaysia, USM fellowship that funded parts of the research discussed in this dissertation.

## TABLES OF CONTENTS

ACKNOWLEDGEMENTS	ii
TABLES OF CONTENTS	iii
LIST OF TABLES	x
LIST OF FIGURES	xiii
LIST OF PLATES	xvii
LIST OF SYMBOLS	xviii
LIST OF ABBREVIATIONS	xx
ABSTRAK	xxv
ABSTRACT	xxvii

### CHAPTER 1: INTRODUCTION

1.1	Background of the study	1
1.2	Problem statement	3
1.3	Research objectives	4
1.4	Scope of study	5
1.5	Organization of the thesis	7

### CHAPTER 2: LITERATURE REVIEW

2.1	Introduction	9
2.2	Bionanotechnology	9
	2.2.1 Ag nanoparticles in bionanotechnology	13
	2.2.2 Antimicrobial properties of silver nanoparticles	17
2.3	Market analysis on Ag nanoparticles	22
	2.3.1 Global market on nanoparticles research	22

2.3.2	Nanotechnology industries in Malaysia	24
2.4	Nanoparticles synthesis and its characteristics	25
2.4.1	Conventional method for Ag nanoparticles synthesis	27
2.4.2	Biological synthesis of Ag nanoparticles	28
2.5	Fungal synthesis of Ag nanoparticles	30
2.5.1	Reduction mechanism of Ag nanoparticles	33
2.5.2	Factors affecting the synthesis of Ag nanoparticles	34
2.6	Filamentous fungi	36
2.6.1	White-rot fungus: <i>Pycnoporus sanguineus</i>	37
2.6.2	Morphology of fungal cell	39
2.6.3	Fungi cultivation in bioreactors	41
2.6.4	Microbial growth	44
2.7	Optimization studies	50
2.7.1	Response surface methodology	50
2.7.2	Box-Behnken design	52

### **CHAPTER 3: MATERIALS AND METHODS**

3.1	Introduction	53
3.2	Chemical and Equipment	53
3.3	Microorganisms	54
3.3.1	White Rot Fungi	54
3.3.2	Bacteria and Fungi for Susceptibility Testing	54
3.4	Research Methodology	54
3.4.1	Cell suspension preparation	56
3.4.2	Cultivation media	56

3.4.3	Production media	57
3.4.4	Cultivation conditions	58
3.4.4 (a)	Shake flask studies	58
3.4.4 (b)	Bioreactor studies	59
3.4.5	Biosynthesis of Ag nanoparticles	60
3.4.6	Statistical experimental design	61
3.4.6 (a)	One-factor-at-a time method	61
3.4.6 (b)	Design of experiment	63
3.4.7	Characterization studies	65
3.4.7 (a)	Surface plasmon resonance	65
3.4.7 (b)	Particle size determination	65
3.4.7 (c)	Particle concentrations	66
3.4.7 (d)	Surface morphology	66
3.4.7 (e)	Particle size and morphology	67
3.4.7 (f)	Functional group determination	67
3.4.8	Antimicrobial Assay	67
3.4.8 (a)	Susceptibility determination	68
3.4.8 (b)	Minimum inhibitory concentration	69
3.4.8 (c)	Minimum bactericidal /fungicidal concentration	69
3.4.9	Analytical method	70
3.4.9 (a)	Biomass determination	70
3.4.9 (b)	Number of spores determination	70
3.4.9 (c)	Glucose determination	71
3.4.9 (d)	Protein concentration and purification	72

3.4.9 (e) Protein determination	72
3.4.9 (f) Polyacrylamide gel electrophoresis	73
3.4.9 (g) In-solution digestion and Nano-LC-Orbitrap	74

## MS/MS

## CHAPTER 4: RESULTS AND DISCUSSIONS

4.1	Screening of Ag nanoparticles producing fungi	76
4.2	Screening of media components for growth of Ag nanoparticles producing fungus	81
4.3	Optimization of growth and protein excretion by <i>P. sanguineus</i> using one-factor-at-a-time (OFAT) method	84
4.3.1	Effect of yeast extract concentration	84
4.3.2	Effect of initial glucose concentration	86
4.3.3	Effect of malt extract concentration	88
4.3.4	Effect of pH	89
4.3.5	Effect of agitation speed	91
4.3.6	Effect of temperature	93
4.4	Optimization studies on protein excretion by <i>P. sanguineus</i> using design of experiment (DoE)	94
4.4.1	Statistical analysis and empirical regression development	96
4.4.2	Effect of process variables on protein excretion	98
4.4.3	Optimization and regression validation	106
4.5	Bioreactor studies on growth of <i>P. sanguineus</i>	109
4.5.1	Effect of aeration	109

4.5.2	Effect of temperature	113
4.5.3	Effect of initial glucose concentration	117
4.5.4	Volumetric mass transfer coefficient of <i>P. sanguineus</i>	120
4.6	Kinetics and modeling for growth, protein excretion, glucose consumption and inhibition by <i>P. sanguineus</i> in a 4L airlift bioreactor	122
4.6.1	Selected empirical model	123
4.6.2	Kinetic parameters estimation	123
4.6.3	Model analysis	124
4.6.3 (a)	Microbial growth	124
4.6.3 (b)	Product formation	128
4.6.3 (c)	Substrate utilization	131
4.6.4	Model validation	134
4.6.5	Inhibition study	136
4.7	Mechanism of Ag nanoparticles synthesis	138
4.7.1	Fourier transmission infrared spectroscopy	138
4.7.2	Sodium dodecyl sulfate- polyacrylamide gel electrophoresis (SDS-PAGE)	142
4.7.3	Protein identification	143
4.8	Ag nanoparticles synthesis in shake flasks studies	145
4.8.1	Effect of surfactants on Ag nanoparticles synthesis	146
4.8.2	Effect of inoculum size on Ag nanoparticles synthesis	148
4.8.3	Effect of AgNO <sub>3</sub> concentrations Ag nanoparticles synthesis	150
4.8.4	Effect of temperature on Ag nanoparticles synthesis	151

4.8.5	Effect of agitation on Ag nanoparticles synthesis	153
4.9	Optimization of Ag nanoparticles synthesis using response surface methodology via Box-Behken	154
4.9.1	Statistical analysis and empirical regression development	155
4.9.2	Effect of process variables on the size of Ag nanoparticles	157
4.9.3	Optimization and model validation	161
4.10	Comparative studies on the Ag nanoparticles synthesis between stirred tank and pressurized reactor	163
4.11	Characterization of Ag nanoparticles	166
4.11.1	Surface plasmon resonance	166
4.11.2	Surface Morphology	168
4.11.3	Energy dispersive X-ray spectroscopy	170
4.11.4	Particle size and morphology	172
4.12	Antimicrobial assay	177
4.12.1	Disc diffusion assay	177
4.12.2	Minimum inhibition concentration, minimum bacterial concentration and minimum fungicidal concentration	180

## **CHAPTER 5 : CONCLUSIONS AND RECOMMENDATIONS**

5.1	Conclusions	185
5.2	Recommendation for future work	188



<b>REFERENCES</b>	190
<b>APPENDICES</b>	226
Appendix A: Chemicals and equipment	232
Appendix B: Standard calibration curves	234
Appendix C: Calculation of cell density using haemocytometer	236
Appendix D: Calibration curve between % pO <sub>2</sub> and C <sub>L</sub>	237
Appendix E: Derivation of Kinetic Models	232
Appendix F: Simulation of experimental data for the determination of kinetic models using Polymath®	237
Appendix G: Particle size obtained from dynamic light scattering	243
<b>LIST OF PUBLICATIONS</b>	245

## LIST OF TABLES

	<b>Title</b>	<b>Page</b>
Table 2.1	Overview of the antimicrobial activity of Ag nanoparticles produced in different sizes	21
Table 2.2	Conventional methods for the synthesis of Ag nanoparticles	29
Table 2.3	List of fungi used for Ag nanoparticles synthesis	32
Table 2.4	Models suggested for microbial growth	45
Table 2.5	Kinetic models for cell growth, product formation, substrate utilization and inhibitions	47
Table 3.1	MYG Media	57
Table 3.2	Production media compositions	57
Table 3.3	Selected components and its concentration for optimization	62
Table 3.4	Selected operating condition and its variable for optimization	62
Table 3.5	Levels of variables chosen for Box-Behnken design for optimization of protein excretion	64
Table 3.6	Levels of variables chosen for Box-Behnken design for optimization of Ag nanoparticles size	64
Table 3.7	Running and stacking gels preparation	73
Table 4.1	Average Ag nanoparticles particles size produced by white-rot fungi in different production mode	79
Table 4.2	Growth media for <i>P. sanguineus</i> as reported in the culture collection procedures	82
Table 4.3	Experimental codes, ranges and level of the independent variables chosen for Box-Behnken design	95
Table 4.4	Box-Behnken design matrix with experimental and predicted values	97
Table 4.5	ANOVA for the quadratic model of the protein excretion during cultivation of <i>P. sanguineus</i>	98

Table 4.6	Optimization criteria at the desired goal for the protein excretion	107
Table 4.7	The Box-Behnken design matrix for model validation and confirmation	108
Table 4.8	Effect of aeration rate on the specific growth rate and protein excretion by <i>P. sanguineus</i> in 8L airlift bioreactor	110
Table 4.9	Effect of substrate concentration on the oxygen uptake rate (OUR), volumetric oxygen transfer coefficient, <i>kLa</i> and oxygen transfer rate (OTR) during cultivation of <i>P. sanguineus</i> in an 8L airlift bioreactor	122
Table 4.10	Estimated model parameters for the growth of <i>P. sanguineus</i> in an 8L airlift bioreactor at different glucose concentrations	126
Table 4.11	Estimated model parameters for the protein excretion in an 8L airlift bioreactor at different glucose concentration	129
Table 4.12	Estimated model parameters for the substrate utilization in an 8L airlift bioreactor at different glucose concentration	132
Table 4.13	Mean square error (MSE) of proposed kinetic models for growth, product formation and substrate utilization at different initial glucose concentration	135
Table 4.14	Estimated parameter values obtained from different substrate inhibition growth models	137
Table 4.15	FTIR peaks and their respective assigned functional groups	140
Table 4.16	Fourier transforms infrared spectroscopy spectra characteristic and functional groups for both functionalized and un-functionalized Ag nanoparticles	141
Table 4.17	Identification of <i>P. sanguineus</i> excreted protein using nanoLC-Orbitrap MS/MS	144
Table 4.18	Experimental codes, ranges and level of the independent variables chosen for Box-Behnken design	155
Table 4.19	Box-Behnken design matrix with experimental and predicted values	156
Table 4.20	ANOVA for the quadratic model of Ag nanoparticles size in the bioreduction of Ag nanoparticles	157

Table 4.21	Optimization criteria to obtain the desired goal for the size of Ag nanoparticles.	162
Table 4.22	Validation and confirmation of response surface analysis	162
Table 4.23	Comparative studies between pressurized and stirred tank reactor in Ag nanoparticles synthesis	165
Table 4.24	Disc diffusion assay between un-optimized and optimized synthesized Ag nanoparticles and the tested antibiotics	178
Table 4.25	MIC, MBC/MFC ( $\mu\text{g/ml} \pm \text{SD}$ ) of Ag nanoparticles showing antimicrobial activities against various pathogens	182
Table E.1	Kinetic models for cell growth	238
Table E.2	Kinetic models for product formation	240
Table E.3	Kinetic models for substrate utilization	241
Table G.1	Particle size and polydispersity index	249

## LIST OF FIGURES

	<b>Title</b>	<b>Page</b>
Figure 2.1	Absorption and scattering spectra of metal nanoparticles based on (a) shape (b) sizes	15
Figure 2.2	Interaction of electromagnetic radiation with metal nanoparticles	16
Figure 2.3	Total market values for nanoparticles in biotechnology, drug development and drug delivery	23
Figure 2.4	Numbers of products associated with specific nanoparticles	24
Figure 2.5	Top-down and bottom-up approaches for nanoparticles synthesis	26
Figure 2.6	Factors influencing nanoparticles characteristics. X shows the ideal nanoparticles characteristic	27
Figure 2.7	UV-vis absorption spectra of Ag nanoparticles at different reaction temperature	35
Figure 2.8	Schematic diagram of airlift bioreactor	42
Figure 2.9	Box-Behnken design	52
Figure 3.1	Research methodology flow chart	55
Figure 3.2	A schematic diagram of an 8 L modified airlift bioreactor (Minifors, Infors-HT, Switzerland)	59
Figure 3.3	Microscopic view of counting chamber in haemocytometer	71
Figure 4.1	Yield of Ag nanoparticles produced by <i>P. sanguineus</i> (PS), <i>S. commune</i> (SC), <i>L. sajar caju</i> (LSC), <i>T. feei</i> (TF) and <i>T. pocas</i> (TP) after 5 days of incubation	80
Figure 4.2	Screening of production media for the growth of <i>P. sanguineus</i>	83
Figure 4.3	Effect of different concentration of yeast extract on cell growth and protein excretion in shake flasks cultures (Condition: 20gL <sup>-1</sup> initial glucose concentration, 10 gL <sup>-1</sup> malt extract concentration, pH 5.6±0.2 , 30°C)	85

Figure 4.4	Effect of different concentration of glucose on <i>P. sanguineus</i> growth and protein excretion in shake flasks cultures. (Condition: 5gL <sup>-1</sup> yeast extract concentration, 10 gL <sup>-1</sup> malt extract concentration, pH 5.6±0.2 , 30°C)	87
Figure 4.5	Effect of different concentration of malt extract on <i>P. sanguineus</i> growth and protein excretion in shake flasks cultures. (Condition: 20gL <sup>-1</sup> initial glucose concentration, 5 gL <sup>-1</sup> yeast extract concentration, pH 5.6±0.2 , 30°C)	89
Figure 4.6	Effect of pH on <i>P. sanguineus</i> growth and protein excretion in shake flasks cultures. (Condition: 20gL <sup>-1</sup> initial glucose concentration, 5 gL <sup>-1</sup> yeast extract concentration, 15 gL <sup>-1</sup> malt extract concentration, 200 rpm, 30°C)	90
Figure 4.7	Effect of agitation speed on cell growth and protein excretion in shake flasks cultures. (Condition: 20gL <sup>-1</sup> initial glucose concentration, 5 gL <sup>-1</sup> yeast extract concentration, 15 gL <sup>-1</sup> malt extract concentration, pH 6.5±0.2, 30°C)	92
Figure 4.8	Effect of temperature on cell growth and protein excretion in shake flasks cultures. (Condition: 20gL <sup>-1</sup> initial glucose concentration, 5 gL <sup>-1</sup> yeast extract concentration, 15 gL <sup>-1</sup> malt extract concentration, pH 6.5±0.2, 150 rpm)	94
Figure 4.9	Normal % probability plot of residual for protein excretion	99
Figure 4.10	Scatter diagram of predicted response versus actual response for protein excretion by <i>P. sanguineus</i>	100
Figure 4.11	Effect of yeast extract and malt concentration on protein excretion by <i>P. sanguineus</i> (Condition: 20 gL <sup>-1</sup> glucose concentration, pH 6.5)	102
Figure 4.12	Effect of glucose and malt extract concentration on protein excretion by <i>P. sanguineus</i> (Condition: 10 gL <sup>-1</sup> yeast extract concentration, pH 6.5)	103
Figure 4.13	Effect of yeast extract concentration and pH on protein excretion by <i>P. sanguineus</i> (Condition: 20gL <sup>-1</sup> glucose concentration, 10 gL <sup>-1</sup> malt extract concentration)	104
Figure 4.14	Effect of glucose concentration and pH on protein excretion by <i>P. sanguineus</i> (Condition: 10gL <sup>-1</sup> yeast	105

	extract concentration, 10 gL <sup>-1</sup> malt extract concentration)	
Figure 4.15	Effect of different aeration rate on cultivation of <i>P. sanguineus</i> in an 8 L airlift bioreactor.	111
Figure 4.16	Effect of different temperature on cultivation of <i>P. sanguineus</i> in an 8 L airlift bioreactor	115
Figure 4.17	Effect of different initial glucose concentration on cultivation of <i>P. sanguineus</i> in an 8L airlift bioreactor	118
Figure 4.18	Response of dissolve oxygen for the determination of OUR and <i>kLa</i> using dynamic gassing out method	121
Figure 4.19	Growth profiles of <i>P. sanguineus</i> at different glucose concentration based on (a) Velhust-Logistic (b) Gompertz and (c) Richard-modified logistic models	127
Figure 4.20	Protein excretion by <i>P. sanguineus</i> at different glucose concentration based on modified Gompertz model	130
Figure 4.21	Kinetic of substrate utilization by <i>P. sanguineus</i> at different glucose concentration based on (a) Logistic-Luedeking-Piret-like (b) Gompertz- modified-Luedeking-Piret-like and (c) First order on-growth associated model (d) Modified Logistic- Luedeking-Piret-like	133
Figure 4.22	Specific growth rates of experimental and simulated data from the inhibition models at different glucose concentration	137
Figure 4.23	FTIR spectrum of mycelia <i>P. sanguineus</i> after the bioreduction of Ag nanoparticles using <i>P. sanguineus</i>	140
Figure 4.24	FTIR spectrum of culture-free Ag nanoparticles before (black) and after (blue) functionalized with SDS	141
Figure 4.25	Proposed synthesis mechanisms of Ag nanoparticles by <i>P. sanguineus</i> through enzymatic reduction of sulfite reductase [NADPH]	145
Figure 4.26	Effect of sodium dedocyl sulphate (SDS) concentration on the size of Ag nanoparticles (Condition: 1 mmol L <sup>-1</sup> AgNO <sub>3</sub> , 200 rpm, 30°C, 1% (v/v) inoculum size)	148

Figure 4.27	Effect of inoculum on Ag nanoparticles size (Condition: 1 mmol L <sup>-1</sup> AgNO <sub>3</sub> , 5 mmol L <sup>-1</sup> SDS, 200 rpm, 30°C)	149
Figure 4.28	Effect of AgNO <sub>3</sub> concentrations on Ag nanoparticles size (Condition: 5 mmol L <sup>-1</sup> SDS, 200 rpm, 30°C, 5% (v/v) inoculum size)	151
Figure 4.29	Effect of temperature on Ag nanoparticles size (Condition: 1 mmol L <sup>-1</sup> AgNO <sub>3</sub> , 1 mmol L <sup>-1</sup> SDS, 200 rpm, 1% (v/v) inoculum size)	152
Figure 4.30	Effect of agitation speed on Ag nanoparticles size (Condition: 1 mmol L <sup>-1</sup> AgNO <sub>3</sub> , 1 mmol L <sup>-1</sup> SDS, 38°C, 1% (v/v) inoculum size)	154
Figure 4.31	Normal % probability plots versus studentized residuals for Ag nanoparticles size	158
Figure 4.32	Scatter diagram of predicted response versus actual response for Ag nanoparticles size	159
Figure 4.33	Three-dimensional response surface graphs on the size of Ag nanoparticles	161
Figure 4.34	UV-vis spectrum for Ag nanoparticles synthesized using <i>P. sanguineus</i> in sample (a) SN and (b) CS	167
Figure 4.35	Spectrum of Ag nanoparticles-free mycelium obtained by EDX spectroscopy, carbon (C), oxygen (O), phosphate(P) and potassium (K)	171
Figure 4.36	Spectrum of Ag nanoparticles synthesized on fungal mycelium obtained by EDX spectroscopy, carbon (C), sodium (Na), chloride (Cl) and silver (Ag)	171
Figure B.1	Glucose concentrations (x) were obtained by substituting the absorbance obtained (y) in the equation.	234
Figure B.2	Protein concentrations (x) were obtained by substituting the absorbance obtained (y) in the equation	234
Figure B.3	Ag concentrations (x) were obtained by substituting the absorbance obtained (y) in the equation	235
Figure D.4	Conversion of % pO <sub>2</sub> to C <sub>L</sub>	237



## LIST OF PLATES

	<b>Title</b>	<b>Page</b>
Plate 2.1	Micro- and nanoworld	10
Plate 2.2	Proposed mechanistic action of Ag nanoparticles on microorganism	20
Plate 4.1	Visual colour observation of synthesized Ag nanoparticles (A) control: containing 1mmol L <sup>-1</sup> AgNO <sub>3</sub> (B) reaction solution: containing Ag nanoparticles after 5 days of incubation	77
Plate 4.2	SDS-PAGE carried out using 12.5% polyacrylamide gel (Lane 1: protein extract; lane 2: protein marker ladder)	142
Plate 4.3	Scanning electron micrograph of the <i>P. sanguineus</i> mycelium (a) before (b) after reaction with 1mmol L <sup>-1</sup> AgNO <sub>3</sub>	169
Plate 4.4	Scanning electron micrograph of Ag nanoparticles synthesized onto the mycelia surface of size >100 nm.	170
Plate 4.5	Top view of fungi mycelia showing Ag nanoparticles deposited on the cell wall membrane at scale 500 nm (20,000 x magnification); arrow showed the location of the Ag nanoparticles	172
Plate 4.6	Cross-sectional views of fungi mycelia at scale 2µm (4,000 x magnification) (b) Zoom view of a section at scale 100 nm (50,000 x magnification); arrow showed the location of the Ag nanoparticles	173
Plate 4.7	TEM micrograph recorded from a drop-coated film of AgNO <sub>3</sub> after reacted with culture-free supernatant of <i>P. sanguineus</i> at a scale of 200 nm (25,000x magnification).	175
Plate 4.8	TEM micrograph recorded from optimized reaction condition of AgNO <sub>3</sub> with culture-free supernatant of <i>P. sanguineus</i> at scale 20 nm (75,000 x magnification).	176
Plate 4.9	Example of disc diffusion assay on <i>S. epidermis</i> using (a) un-optimized and (b) optimized Ag nanoparticles	180

## LIST OF SYMBOLS

$\alpha$	Product formation constant	
$\beta$	Product formation constant	
$\sigma$	Variance	
$\varphi_r$	Fractional gas holdup of riser	
$\Phi_d$	Fractional gas holdup of downcomer	
$\mu\text{L}$	Millilitre	
$n$	Constant	
$r$	Constant	
$X_i$	Input variables	
$Y$	Predicted response	
$\mu$	Specific growth rate	$\text{h}^{-1}$
$\emptyset$	Diameter	$\text{m}$
$\varepsilon$	Dielectric permittivity	$\text{F/m}$
$\rho$	Density	$\text{gcm}^{-3}$
$\tau_i$	Residence time for liquid	$\text{S}$
$\Delta P_b$	Pressure difference	$\text{kPa}$
$a_i$	Specific interfacial area	$\text{m}^2$
$C$	Concentration	$\text{molL}^{-1}$
$C^*$	Saturation concentration	$\text{molL}^{-1}$
$C_L$	Dissolved oxygen concentration	$\text{molL}^{-1}$
$D$	Diffusion coefficient for growth limiting nutrient	$\text{cm}^2 \text{s}^{-1}$
$E_a$	Activation energy	$\text{kJmol}^{-1}$

$g$	Gravitational constant	$\text{ms}^{-2}$
$G_s$	Gas production	$\text{Ls}^{-1}$
$h_i$	Effective length	$\text{M}$
$k_L$	Mass transfer coefficient	$\text{m h}^{-1}$
$k_d$	Death rate	$\text{h}^{-1}$
$\text{kHz}$	Kilohertz	$\text{s}^{-1}$
$k_{La}$	Mass transfer coefficient	$\text{m s}^{-1}\text{m}^2$
$L_{O_2}$	Oxygen solubility	$\text{mol L}^{-1}$
$\text{mA}$	Milliampere	$\text{C s}^{-1}$
$\text{mM}$	Millimolar	$\text{mmol L}^{-1}$
$M_o$	Initial biomass	$\text{g}$
$\text{OTR}$	Oxygen transfer rate	$\text{molL}^{-1}\text{s}^{-1}$
$P$	Product concentration	$\text{g L}^{-1}$
$P_a$	Atmospheric pressure	$\text{kPa}$
$P_b$	Pressure at the bottom bioreactor	$\text{kPa}$
$Q$	Specific utilization rate of the growth limiting nutrient	$\text{s}^{-1}$
$Q_L$	Gas flowrate	$\text{m}^3\text{s}^{-1}$
$R$	Radius	$\text{m}$
$R$	Universal gas constant	$\text{Jmol}^{-1}\text{K}^{-1}$
$S$	Substrate concentration	$\text{gL}^{-1}$

vvm	Volume of air per unit medium per minute	$\text{LL}^{-1}\text{min}^{-1}$
W	Width of active outer mycelia shell.	cm
X	Biomass concentration	$\text{gL}^{-1}$

### LIST OF ABBREVIATIONS

8MP	Eight Malaysian Plan
AAS	Atomic absorption spectroscopy
ADP	Adenosine diphosphate
ANOVA	Analysis of variance
APS	Ammonium persulfate
ATCC	American Type Culture Collection
ATP	Adenosine triphosphate
BBD	Box-behnken Design
BES	The Office of Basic Energy Sciences
C/N	Carbon to nitrogen
$C_{\text{ext}}$	Total cross section of light absorption and scattering
CAGR	Compound Annual Growth Rate
CAHs	Chlorinated aromatic hydrocarbons
CD4	Cluster of differentiation 4
CFU	Colony forming unit
$C_p$	Replicate number
CS	Fungi-secreted protein in culture supernatant
CTAB	Cetyl trimethylammonium bromide

CySH	Cystein
DDT	Dichlorodiphenyltrichloroethane
DLS	Dynamic light scattering
DNA	Deoxyribonucleic acid
DNS	Dinitrosalicylic solution
DO	Dissolved oxygen
DoE	Design of experiment
DSMZ	Deutsche Sammlung von Mikroorganismen und Zellkulturen
EC50	Half effective concentration
EDEX	Energy dispersive X-ray
EFTEM	Electron field transmission electron microscopy
FESEM	Field emission scanning electron microscopy
FRIM	Forest Research Institute of Malaysia
FTIR	Fourier transform infrared spectroscopy
gp120	Envelope glycoprotein
gp41	Glycoprotein 41
H1N1	Influenza A virus
HAADF	High angle annular dark field
HBV	Hepatitis B virus
HIV	Human immunodeficiency virus
HPLC	High performance liquid chromatography
HrP	Horseradish peroxidase
IR	Infrared
IRPA	Priority research area
k	Factor number

kDa	Kilodalton
$K_L$	Substrate inhibition constant
$K_p$	Product inhibition constant
$K_s$	Half saturation constant
LC-MS/MS	Liquid Chromatography- tandem Mass Spectrometry
LD50	Median lethal dose
LiP	Lignin peroxidase
LSW	Lifshitz–slyozov–wagner
MBC	Minimum bactericidal concentration
MEA	Malt extract agar
MFC	Minimum fungicidal concentration
MGH	Massachusetts general hospital (mgh)
MIC	Minimum inhibition concentration
MnP	Manganese peroxidase
MOSTI	Ministry of Science, Technology and Innovation
MP	Absorption of silver atom on the mycelia pellet
$m_s$	Maintenance energy
MS	Mass spectroscopy
MSE	Mean squares error
MWCO	Molecular weight cut-off
MYG	Malt extract-yeast extract-glucose
NAD	Nicotinamide adenine dinucleotide
NADP	Nicotinamide adenine dinucleotide phosphate
NADPH	Nicotinamide adenine dinucleotide phosphate
ND	Not determined

NIBS®	Non-invasive back scatter
NND	National nanotechnology directorate
NNI	National nanotechnology initiative
OFAT	One-factor-at-one-time
OTR	Oxygen transfer rate
OUR	Oxygen uptake rate
PAHs	Poly-aromatic hydrocarbons
PBS	Phosphate buffer saline
PDI	Polydispersity index
PEN	Project on Emerging Nanotechnologies
pH	Hydrogen-ion concentration
pO <sub>2</sub>	Partial dissolved oxygen
R <sup>2</sup>	Determination coefficient
RAPET	Reaction under autogenic pressure at elevated temperatures
RNA	Ribonucleic acid
rpm	Rotation per minutes
RSM	Response surface methodology
SD	Standard deviation
SDS	Sodium dedocyl sulfate
SDS-PAGE	Sodium dedocyl sulfate-polyacrylamide gel electrophoresis
SEC	Size-exclusion chromatography
SEM	Scanning electron microscopy
SERS	Surface-enhanced Raman spectroscopy
-SH	Thiol group
SN	The mycelia pellet which was released into the silver nitrate

$S^{\circ}$	Maximum substrate concentration
SPR	Surface Plasmon resonance
STM	Scanning tunnelling microscope
TEM	Transmission electron microscopy
TEMED	N, N, N', N'-tetramethylethylenediamine
Tris	2-Amino-2-hydroxymethyl-propane-1,3-diol
UV-vis	Ultraviolet visible
$Y_{x/s}$	Yield of biomass over substrate



# PENGAYAAN PROTEIN OLEH *PYCNOPORUS SANGUINEUS* UNTUK SINTESIS ZARAH NANO-AGENTUM

## ABSTRAK

Pengawalan saiz nanobahan telah menarik perhatian kerana sifatnya yang unik untuk mencapai sesuatu proses, terutamanya dalam aplikasi biologi dan perubatan. Dalam konteks ini, unsure agendum (Ag) yang mempunyai kesan antimikrob yang baik, adalah penting. Pendekatan yang mudah dan berkesan untuk sintesis zarah nano-agentum dengan mekanisme pengurangan protein yang dihasilkan oleh beberapa spesies kulat reput putih telah dikaji. *Pycnoporus sanguineus* telah didapati boleh menghasilkan saiz zarah nano Ag yang terkecil dengan tahap “*monodispersity*”. Rekabentuk Box-Behnken telah diguna untuk mengoptimumkan media fermentasi untuk penghasilan protein dengan kulat yang dipilih. Empat pembolehubah yang terlibat dalam kajian ini ialah glukosa, ekstrak malt, ekstrak yis dan pH. Media yang optimum mengandungi 8.39 gL<sup>-1</sup>, 18.34 gL<sup>-1</sup>, 14.71 gL<sup>-1</sup> daripada ekstrak yis, glukosa dan ekstrak malt masing-masing pada pH 6.66 dengan menghasilkan protein maksimum pada 0.858 gL<sup>-1</sup>. Pertumbuhan kinetik kulat, penggunaan glukosa dan pembentukan produk juga telah dilaporkan. Keputusan menunjukkan bahawa pada kepekatan glukosa awalan 20gL<sup>-1</sup>, model “*Richard-modified logistic*” (R<sup>2</sup> =0.9839) untuk pertumbuhan mikrob, model “*modified Gompertz*” (R<sup>2</sup> =0.9610) untuk pembentukan produk dan model “*first order non-growth associate*” (R<sup>2</sup> =0.9736) untuk penggunaan glukosa adalah berpadanan dengan data eksperimen. Strategi pengoptimuman berurutan berdasarkan kaedah satu factor pada satu masa (OFAT) dan rekabentuk statistik eksperimen telah digunakan untuk mengoptimumkan parameter bagi meningkatkan penghasilan zarah nano Ag. Berdasarkan kaedah OFAT, tiga faktor penting yang mempengaruhi saiz zarah nano-agentum telah

dikenal pasti sebagai kepekatan  $\text{AgNO}_3$ , suhu pengeraman dan kelajuan pengadukan. Nilai optimum pembolehubah bagi proses sintesis zarah nano Ag ditentu dengan menggunakan kaedah sambutan permukaan (RSM) berdasarkan rekabentuk Box-Behnken. Kesahihan model ini dibangun telah disahkan dan analisis statistik menunjukkan bahawa keadaan operasi yang optimum adalah pada  $1\text{mmolL}^{-1}$   $\text{AgNO}_3$ ,  $40^\circ\text{C}$  dan 230 rpm dengan saiz zarah nano Ag yang terkecil pada 7.58 nm. Perbandingan kajian di dalam reactor teraduh dan reactor bertekan telah dijalankan untuk sintesis zarah nano Ag. Didapati bahawa lebih kecil saiz zarah nano Ag (8.52 nm) yang dihasilkan pada tekanan operasi yang tinggi (10 bar) dan suhu ( $150^\circ\text{C}$ ). Pencirian zarah nano yang telah dihasilkan kemudiannya dianalisa dengan menggunakan spektroskopi UV-vis, DLS, FTIR, TEM, dan SEM. Keputusan menunjukkan bahawa jalur penyerapan zarah nano Ag terletak di puncak 420 nm. Aktiviti antimikrob oleh zarah nano Ag yang dihasilkan telah ditentu dengan menggunakan kaedah difusi cakera, dan kaedah kepekatan bakteria dan kulat minimum. Keputusan mencadangkan bahawa zarah nano Ag yang dihasil dengan menggunakan keadaan yang optimum mempunyai aktiviti antimikrob yang lebih tinggi berbanding dengan zarah nano Ag yang disintesi dengan keadaan tidak optimum. Mekanisme bio-pengurangan zarah nano Ag telah dikaji dan dicadangkan bahawa enzim sulfit reductase [NADPH] telah berperanan untuk bio-pengurangan zarah nano Ag. Ini menunjukkan bahawa enzim dirembeskan oleh *P. sanguineus* bertanggungjawab sebagai agen penurunan yang mampu untuk mensintesis zarah nano Ag dengan saiz kurang daripada 10 nm.

# PROTEIN ENRICHMENT OF *PYCNOPORUS SANGUINEUS* FOR SILVER NANOPARTICLES SYNTHESIS

## ABSTRACT

Controlling sizes of nanomaterials are attracting a great deal of attention because of their unit properties for achieving specific processes especially in biological and medical applications. In this context, Ag which possesses good antimicrobial effects is of interest. A simple and effective approach for the synthesis of Ag nanoparticles by reduction mechanism of proteins synthesized by several species of white rot fungi was studied. *Pycnoporus sanguineus* was found to produce smallest Ag nanoparticles with degree of monodispersity. A Box-Behnken design was employed to optimize a fermentation medium for the production of protein by the selected fungi. The four variables involved in the study were glucose, malt extract, yeast extract and pH. The optimized medium contained 8.39 gL<sup>-1</sup>, 18.34 gL<sup>-1</sup>, 14.71 gL<sup>-1</sup> of yeast extract, glucose and malt extract respectively with initial pH 6.66; and produced the maximum protein at 0.858 gL<sup>-1</sup>. Kinetic growth of the fungi, glucose consumption and product formation of the tested fungus were also reported. It is showed that at initial glucose concentration of 20gL<sup>-1</sup>, Richard-modified logistic model (R<sup>2</sup> =0.9839) for microbial growth, modified Gompertz model (R<sup>2</sup> =0.9610) for product formation and first order non-growth associate (R<sup>2</sup> =0.9736) for glucose consumption were fitted well with the experimental data. Sequential optimization strategy based on one-factor-at-a-time (OFAT) method and statistical experimental design were employed to optimize the process parameters for the enhancement of Ag nanoparticles synthesis. Based on the OFAT method, three significant factors influencing the size of Ag nanoparticles such as AgNO<sub>3</sub> concentration, incubation temperature and agitation speed. The optimum values of these process parameter for

the synthesis of Ag nanoparticles were determined using response surface methodology (RSM) based on Box-Behnken design. The validity of the model developed was verified and the statistical analysis showed that the optimum operating conditions were  $1\text{mmolL}^{-1}$  of  $\text{AgNO}_3$ ,  $40^\circ\text{C}$  and 230 rpm with the smallest Ag nanoparticles produced at 7.58 nm. Comparative studies were conducted for the synthesis of Ag nanoparticles in a stirred tank and a pressurized reactor. It was observed that smaller Ag nanoparticles sizes (8.52 nm) were produced at high operating pressure (10 bar) and high operating temperature ( $150^\circ\text{C}$ ). The synthesized Ag nanoparticles were characterized using UV-vis spectroscopy, DLS, FTIR, TEM, and SEM. Results showed that Ag nanoparticles absorption band was located at a peak of 420 nm. Antimicrobial activities of Ag nanoparticles synthesized have been determined using disc diffusion method, and minimum bactericidal and fungicidal concentration method. The results suggested that Ag nanoparticles synthesized using the described optimum conditions have higher antimicrobial activities compared to the Ag nanoparticles synthesized from non-optimized condition. The bioreduction mechanism of Ag nanoparticles was studied and it was observed that proposed enzyme sulfite reductase [NADPH] was found to be responsible for the bioreduction of Ag nanoparticles. Thus, showing that, enzyme secreted by *P. sanguineus* served as a reducing agent which capable to synthesize Ag nanoparticles with size less than 10nm.

## CHAPTER ONE

### INTRODUCTION

#### 1.1 Background of the study

Nanoparticles are engineered nanomaterials that are created through nanotechnology, a technology which manipulates matters at an atomic or molecular scale to form particles of nanosizes. Recently engineered nanomaterials have drawn a considerable attention. Engineered nanomaterials often have sizes in the range of 1-100 nm. As the size of particles decreased into nanosizes, it had manifested on the physical and chemical properties over the bulk materials (Chulovskaya and Parfenyuk, 2009) such as a high surface to volume ratio, high reactivity, surface energy and spatial confinement (Klabunde *et al.*, 1996). Due to the unique physiochemical characteristic that nanoparticles possessed, they are highly utilized in various industries.

Among the noble nanoparticles, Ag nanoparticles is in much demand for its conductive application in electronic industries such as in semiconductors (Schmid and Hornyak, 1997), superconductors (Henglein, 1993), super magnets (Lee *et al.*, 1995), and micro-electronics (de Heer, 1993). Besides, Ag nanoparticles were also used efficiently in optical applications for enhancing optical spectres and fluorescence (Liz-Marzán, 2005), surface-enhanced Raman scattering (Cao *et al.*, 2003) and localized surface Plasmon resonance (Endo *et al.*, 2010; Misra *et al.*, 2013). One of the fast growing Ag nanoparticles sector now is in the creation of biocompatibility antimicrobial products such as antibacterial water filters (Jain and Pradeep, 2005), biosensors (Wu *et al.*, 2006), biocatalyst (Wang, 2006), catheters

and prostheses for prevention of bacterial colonization (Gosheger *et al.*, 2004; Samuel and Guggenbichler, 2004), and nano-engineering in therapeutic drug delivery (Zhang *et al.*, 2008).

Engineered nanoparticles are of major interest as a result of the rapid development in nanotechnology. Engineered nanoparticles can be made from different materials such as phospholipid, chitosan, polymers, carbon, silica and various metals (De Jong and Borm, 2008) and are designed to form different shapes including solid spheres, hollows, tubes, rods, and complex strands. Among the metal nanoparticles, silver has been used since prehistoric times for the treatment of burns as reported by Chung and Herbert (2001).

Green synthesis of nanoparticles is an emerging branch of nanotechnology in which it uses the environmental benign materials. Besides, it also offers numerous benefits of eco-friendliness and compatibility for biomedical applications. The revolution of nanotechnology has studied the photophysical attributes of Ag nanoparticles and efficient addressability via a rare combination of valuable properties namely, optical properties associated with surface plasmon resonance, well developed surfaces, catalytic activity, high electrical double layer capacitance, etc. (Henglein, 1993). The fundamental studies of Ag nanoparticles have brought them to the forefront of bionanotechnology research towards the applications of biomedicine (Nair and Laurencin, 2007).

## 1.2 Problem statement

Various physical and chemical methods have been used extensively on industrial scale to produce monodispersed nanoparticles. The use of toxic chemicals and their stability are of vital concerns. Toxic chemicals are used on the surface of nanoparticles and as non-polar solvents during nanoparticles synthesis. However the used of toxic chemicals is not suitable in clinical fields. Synthesizing nanoparticles using a green, bottom-up approach, which is regarded as safe, eco-friendly, cost-effective and sustainable is the way forward.

Besides that, the increasing resistance of microbial organisms to multiple antibiotics and the continuing emphasis on lower healthcare costs has spurred many researchers to develop new, effective reagent-free antimicrobial at a lower cost. Such problems and needs have led to the resurgence in the use of silver-based antiseptics that are linked to broad-spectrum activity and far lower propensity to induce microbial resistance than antibiotics (Jones *et al.*, 2004).

According to Silver and Phung (1996), antibacterial effects of silver salts have been noticed since ancient times; and silver is now used to control bacterial growth in a variety of applications including dental-related works, catheters and burn wound treatment (Catauro *et al.*, 2004). In fact, it is well known that silver ions and silver-based compounds, with their strong biocidal effects, were highly toxic to microorganisms such as *E. coli* (Zhao and Stevens, 1998). A report by Aymonier *et al.* (2002) has shown that hybrids of Ag nanoparticles with amphiphilic hyper branched macro-molecules exhibited effective antimicrobial surface coating agent.

As the demand for Ag nanoparticles increases, it is crucial to determine a cost effective, large scale and eco-friendly green synthesis method to synthesize Ag

nanoparticles. Even though there are many green synthesis methods for the production of Ag nanoparticles, there has been no publication on the synthesis of Ag nanoparticles by locally isolated white rot macro fungi; neither were the effects of antimicrobial activity involved on the inhibition against various disease-causing microorganisms nor the mechanisms of Ag nanoparticles synthesis by microorganisms. Publications on large scale production of Ag nanoparticles, cultivation mode for optimum production of Ag nanoparticles in bioreactors are limited. This research will provide an alternative to the industry to produce Ag nanoparticles biologically. On the other hand, there are many proposed mechanisms of Ag nanoparticles synthesis by fungi strains (Ottow and Von Klopotek, 1969; Durán *et al.*, 2005), but the exact mechanism of action on how Ag nanoparticles is produced through microbial synthesis is still not known. The use of proteomics work such as SDS-PAGE, HPLC, and LC-MS/MS further confirmed the synthesis reaction of Ag nanoparticles by the selected fungi.

### **1.3 Research objectives**

The measurable objectives are as follow:

- (a) To screen the capability of the selected fungus for Ag nanoparticles synthesis in shake flask cultures
- (b) To optimize the process variables for growth and protein excretion by selected fungus through statistical optimization and kinetics studies of the selected fungus in an airlift bioreactor.



- (c) To optimize the synthesis of Ag nanoparticles in shake flasks using statistical tools and comparative studies of Ag nanoparticles synthesis in a stirred tank and pressurized reactor.
- (d) To study the synthesis mechanism, characterization and antimicrobial activities of the synthesized Ag nanoparticles.

#### **1.4 Scope of study**

Different species of white rot fungi were screened by cultivating them in malt extract nutrient broth at 30°C, 200 rpm for 3 days, and then challenged with silver nitrate solution (1mM, 30°C, 200 rpm, and 5 days) for the bioreduction process. In Ag nanoparticles synthesis, different synthesis routes were studied such as:

- (a) bioreduction of silver ion in the cell free culture supernatant
- (b) bioreduction of silver ion by absorption of silver atom on the mycelia pellet
- (c) bioreduction of silver ion from the mycelia pellet which was released into the silver nitrate solution

The species that showed the highest production of Ag nanoparticles was selected for further analysis. In order to identify the bio-reducing molecules that were present in the reactions, the cell culture was subjected to protein separation and purification using size-exclusion chromatography column, and sodium-dodecyl sulphate-polyacrylamide gel electrophoresis (SDS-PAGE). Next, the positive fraction was then analyzed by an orbitrap nano LC-MS/MS system.

Various analytical tools were used to characterize the synthesized Ag nanoparticles either in the form of intracellular or extracellular, such as UV-vis spectrophotometer, dynamic light scattering, atomic absorption spectrophotometer,

scanning electron microscopy, energy dispersive X-ray spectroscopy, and transmission electron microscopy.

For optimization studies, a one-factor-at-one-time (OFAT) method and a design of experiment (DoE) were employed. OFAT was used as a preliminary step to determine the influencing factors before subjecting each factor to a statistical analysis. In fungal cultivation, glucose, yeast extract, malt extract and pH were selected as the influencing factors for growth and protein excretion. For Ag nanoparticles synthesis, the variables studied were stabilizer concentration, AgNO<sub>3</sub> concentration, inoculum percentage, temperature and agitation. For statistical analysis, a Design Expert software version 6.1.10, (State-Ease, Inc, USA) was used for the analysis of DoE. In this method, all variables obtained from OFAT were varied simultaneously according to the set of experimental runs generated by the software using response surface methodology (RSM) coupled with Box-Behnken design (BBD).

To describe the kinetics of Ag nanoparticles producing fungus in an air-lift bioreactor, different kinetics models for microbial growth, product formation, glucose consumption and inhibition study were selected. These models were then validated using the correlation of coefficient ( $R^2$ ) and mean square error (MSE). Models with the best fitted experimental data were then chosen as the working models.

Several process studies were performed on the synthesis of Ag nanoparticles. Ag nanoparticles were first synthesized in shake flasks and then the optimized conditions obtained were then used in reactors (pressurized reactor and stirred tank reactor) synthesis. The Ag nanoparticles synthesis was performed in a 8L reactor with controlled temperature and agitation speed. Later, the process was then

compared with synthesized Ag nanoparticles in a pressurized reactor of varied temperatures (38°C & 150°C) and pressures (1 bar & 10 bar). The process which synthesized Ag nanoparticles in the most effective way was suggested as the best scale-up process in Ag nanoparticles synthesis.

## **1.5 Organization of the thesis**

The first chapter introduces the Ag nanoparticles, the available synthesis method followed by determination of research objectives and scope of study for this research project.

Chapter two gives further insight on the capability of white-rot fungi in Ag nanoparticles synthesis, reviews on the methods for synthesis of Ag nanoparticles. The multi-disciplinary studies on bionanotechnology and the applications of Ag nanoparticles are also discussed. Characterization techniques used for the analysis are elaborated. Reviews of kinetics and modeling of process studies will also be presented.

In materials and methods (Chapter three), list of all materials and chemical used in the research are listed. Detailed procedures for the fungus cultivation and Ag nanoparticles synthesis are presented. This chapter also illustrates comprehensively the analytical methods used in both identification of bio-reducing molecules and characterization of the synthesized Ag nanoparticles.

Chapter four discusses all the experimental data obtained. Firstly, the selection of white-rot fungi species and production routes of Ag nanoparticles are presented. It is then followed by the characterization studies of synthesis of the Ag nanoparticles. Discussion on the bioreduction mechanism of Ag nanoparticles by

biomolecules and mechanistic action of Ag nanoparticles on microbial system are also presented. Statistical methods used to determine the effect of interaction between process variables towards the responses and optimization of the responses will be discussed. The most effective way in large-scale production of Ag nanoparticles will also be reported.

Chapter five concludes concisely all the major findings in this present research work. Suggestions and future recommendations are also presented for future studies.

## **CHAPTER TWO**

### **LITERATURE REVIEW**

#### **2.1 Introduction**

This section reviews the potential of Ag nanoparticles in bionanotechnology and the use of Ag nanoparticles in various industries. The literatures regarding the biosynthesis of Ag nanoparticles by fungi are also presented. This chapter also reviews the various approaches reported for the elucidation of the kinetics of fungi cultivation and Ag nanoparticles formation.

#### **2.2 Bionanotechnology**

Nanotechnology involves science and technology that manipulate precisely matters at nano-scale. It forms the bridge between different disciplines including engineering, chemistry, electronics, etc. with the concern of bringing the existing technologies to nano-scale (Battard, 2012). The term nanotechnology draws its name from the prefix “nano”. It comes from the Greek word “nanos” meaning “a dwarf”. Hence nanotechnology refers to the technology in applying materials or devices with characteristic length scales less than 100 nm. In 2011, the Office of Basic Energy Sciences (BES) for the U.S. Department of Engineering gave illustration between the micro- and nanoworld by comparing the natural and manmade materials in the title “The Scale of Things” as shown in Plate 2.1.

## The Scale of Things – Nanometers and More

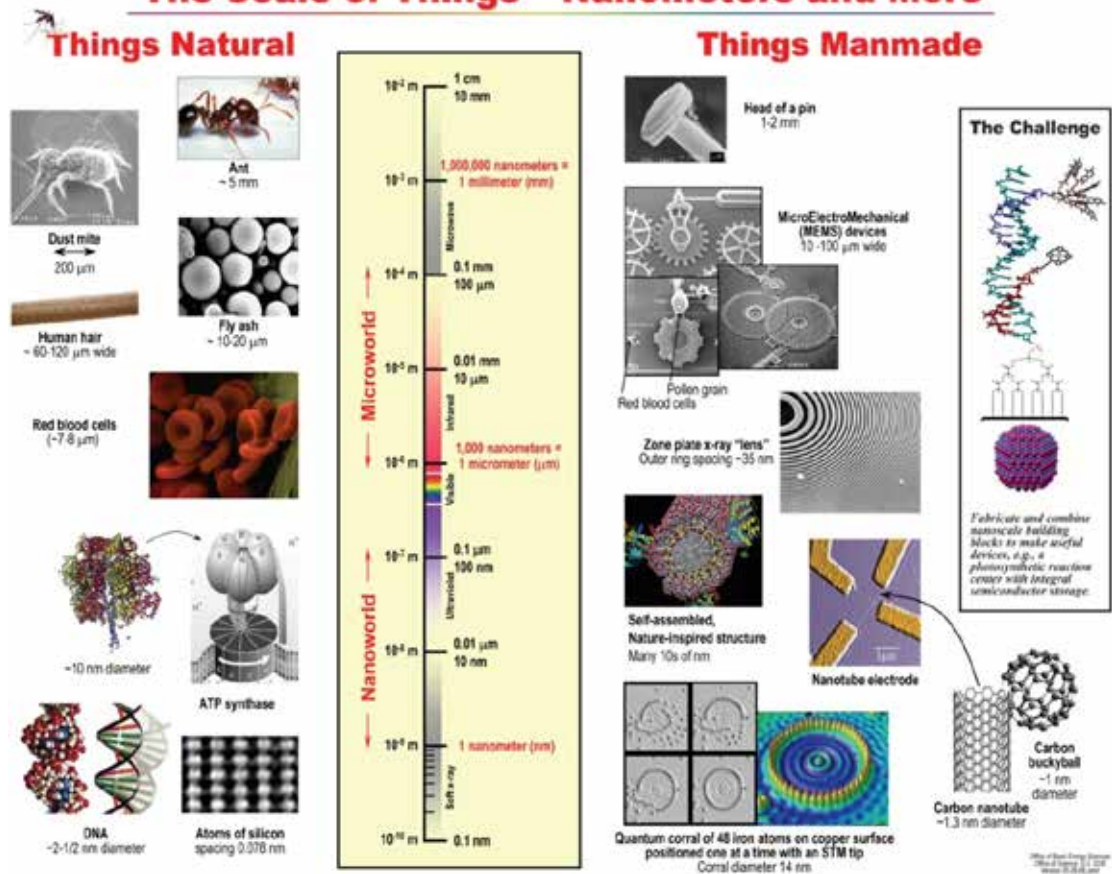


**Plate 2.1** Micro- and nanoworld

(Source: Office of Basic Energy Science, US Department of Energy, <http://science.energy.gov/bes/news-and-resources/scale-of-things-chart/>)

The basic concept of nanotechnology was first described by Nobel Prize winning physicist, Richard Feynman in 1959 in his talk “There’s Plenty of Room at the Bottom” (Feynman, 1992). Later, Taniguchi coined the term “nano-technology” to describe ion-sputter machining (Taniguchi, 1974). Then, nanotechnology had evolved from a concept to rigid technology by the birth of cluster science and the invention of the scanning tunnelling microscope (STM). Nanotechnology is now advancing with production of evolutionary nanotechnology products and processes such as carbon nanotubes, nanocomposites, nanoparticles, nanopatterning, quantum dots for medical imaging, etc. (Fu *et al.*, 2005; Khosravi-Darani *et al.*, 2007;

Sakamoto *et al.*, 2010; Jaganathan and Godin, 2012). Today, with the revolution of nanotechnology, the cross marriage between molecular biology and nanotechnology has been introduced.

In the biomedical context, bionanotechnology are consider a pragmatic approach as nanotechnology through biotechnology (Sarikaya *et al.*, 2003) such as engineered nanostructures and nanomachines or naturally occurring cell machinery with submicron biological molecules such as proteins, peptides, DNA, RNA in a living organism (Zahid *et al.*, 2013). The self-assembling nature of biological macromolecules such as protein, peptide, etc is important for the engineered nanostructure of molecular templates and supra-molecular structures (Zhang, 2003). The self-assembly biomolecules are crucial in recognizing complementary regions where it is a base for the binding and building of tissues and organs from these biomolecules. Most of the biomolecules such as proteins are amphiphile in nature; resulting the high biocompatibility for attachment to various materials because they could maintain their structure and conformation in both hydrophilic and hydrophobic environments (Kiselev, 2006). The wide physiological diversity, small size, genetic manipulability and controlled culturability, microbial cells are an ultimate nanofactory for the production of engineered nanostructure, materials and instruments in bionanotechnology (Villaverde, 2010).

It is frequently observed that most features or characteristics of nanoparticles are size-dependent. Therefore, the properties of nanoparticles are enhanced and modified as its nanosize is scaled down further. Although nanoparticles seem to have desirable advantages, the disadvantages are seen with the revolution of bionanotechnology. Cancer therapy becomes possible with bionanotechnology however; the cost of treatment becomes expensive and is hardly affordable to

patients. Direct injection of nanoparticles into the blood stream is worrying as there is still unknown side-effects to the patients (Lara *et al.*, 2009). A dilemma occurs with developing technology-intensive treatment, they are inaccessible to patients who need them most. In a nutshell, bionanotechnology is a life enhancing advancement. Intensive investigations are required to put bionanotechnology into the hands of the end-user, such as looking into cost-effective production and commercialization, and making bionanotechnology safer by subjecting nanodrug candidates to clinical trials.

The director of the Centre for System Biology at Massachusetts General Hospital (MGH), Dr. Weissleder has developed systematic way to explore disease biology using bionanotechnology (Bogdanov Jr *et al.*, 1999; Jaffer *et al.*, 2006a; Jaffer *et al.*, 2006b). Also, Nadarajah (2009) refers bionanotechnology as “pedestrian applications” of a very powerful science. Some really interesting work is happening in the medical industry. For example, Ag nanoparticles have shown to have better antimicrobial activity against bacteria, yeast and fungus where currently there are publications confirming that Ag nanoparticles (Elechiguerra *et al.*, 2005; Lara *et al.*, 2010) and nano-emulsion (Rueter, 2008) vaccines can exert antiviral activity against HIV-1. Thus, it is believed that bionanotechnology is a new area especially in medical application for antimicrobial and antiviral diseases.

Researchers from Stanford Center for Magnetic Nanotechnology conducted researches on the incorporation of computer chips inside living cells (Xu *et al.*, 2008b; Gaster *et al.*, 2011) which is the future area of bionanotechnology. As biological processes occur inside cells and are greatly important in biomedicine and in biological traceability, development of nano-chips in living cells could help in understanding the biochemical and transport processes at cellular level. A more



challenging area of bionanotechnology in medical application would be cancer therapy. After decades of clinical trials, recently there were evidences that therapies based on bionanotechnology have been effective in humans (Garcia-Bennett *et al.*, 2011; Gou *et al.*, 2011; Lee and Wong, 2011). Researchers also demonstrated that increasing the amount of nanoparticles injected into human bloodstreams increased the efficiency of the treatment. However, the researches on cancer and bionanotechnology are related more to diagnosis and therapy. In the near future, nanodiagnostic devices could revolutionize the biomedical industry.

### **2.2.1 Ag nanoparticles in bionanotechnology**

There are basically three types of nanoparticles: metallic, semiconductor and polymeric nanoparticles (Liu, 2006). They display fascinating properties which differ from those of individual atoms, surfaces or bulk materials. Metallic nanoparticles include gold nanoparticles and nanoparticles which are produced from magnetized metals such as iron, nickel, cobalt etc. As magnetized nanoparticles are produced from magnetized bulk metals, they have the ability to manipulate external magnetic field gradient which is very useful in identifying biomolecules. Quantum dot refers to semiconductors in nanosize whose excitons are confined in all three spatial dimensions (Fu *et al.*, 2005). The unique properties of fluorescence have been studied. Even though the size-dependent photostability properties have been discovered by Efros *et al.* (1996), water insolubility properties of quantum dot is a challenge towards biocompatibility issue associated with biological molecules. Recently, many studies have been conducted to overcome this issue which will be discussed further. Biological molecules which are nanosize such as dendrimers and liposomes are classified as polymeric nanoparticles. Dendrimers are complex

molecule with very well-defined chemical structures which are nearly perfect monodisperse and highly branched in three dimensional structures. Biologically inert properties of dendrimers create the interest in pharmaceutical and biomedical applications which act as a multifunctional nanodevice.

Ag nanoparticles are of concern due to its optical and antimicrobial properties. The optical properties of Ag has been studied for diagnosis and imaging in biomedical application. The remarkable optical properties of Ag nanoparticles are related to the localized plasmon resonance which lies in the visible spectral range (Haes and Van Duyne, 2002). It was reported that the frequency of surface plasmon resonance depends on several factors such as shape, size, dielectric constant of metal nanoparticles, interparticles interaction and electron density (Jain *et al.*, 2006) . The characteristic feature of absorption band and scattering spectra of Ag nanoparticles of different shapes and sizes are illustrated in Figure 2.1. It was observed that the absorption band of metal nanoparticles is located in the visible range or in the adjacent near-IR and UV region. This band is known as surface plasmon resonance (SPR) or the Mie resonance. Ag nanoparticles have shown to exhibit highest extinction ratio in the SPR band peak among all metals and materials that are known to absorb in the same spectral range (Yu *et al.*, 2008). The SPR band occurred as a result of the interaction of light on the nanoparticles surface with the conduction electrons of the metals (Xia and Campbell, 2007).

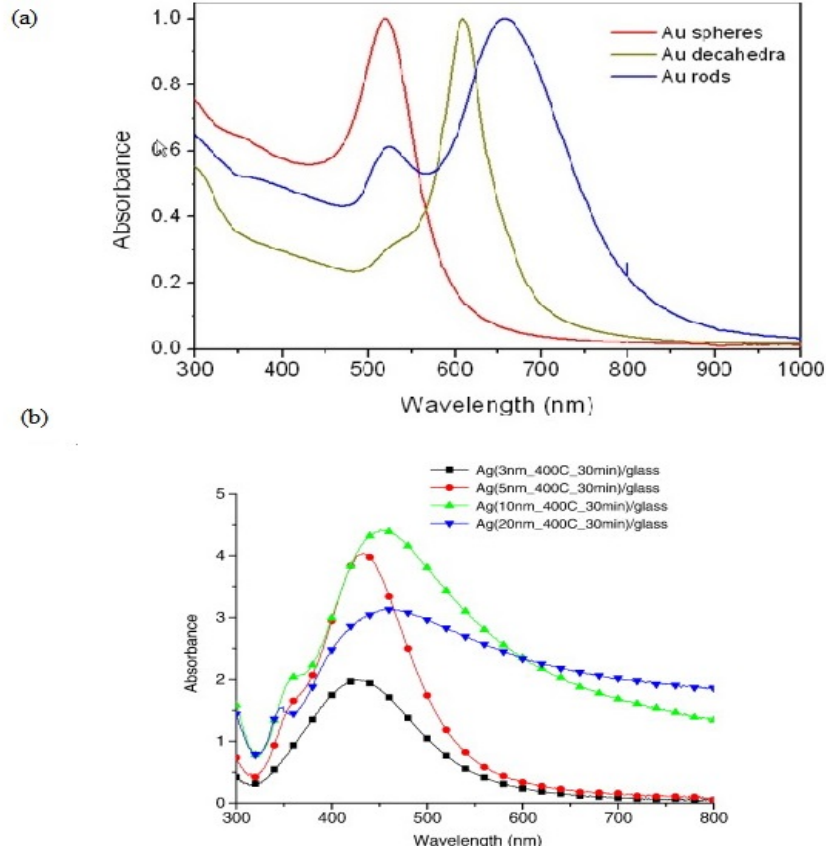


**Figure 2.1** Absorption and scattering spectra of metal nanoparticles based on (a) shape (Liz-Marzán, 2007), (b) sizes (Lee *et al.*, 2008)

In the electron-gas theory, the core electrons are localised at the atomic nucleus while the outer electron are mobile within the metal particles. By alternating the electric field, the mobile conduction electrons are shifted as illustrated in Figure 2.2. The total cross-section of light absorption and scattering by a particle ( $C_{ext}$ ) was described in Mie theory (Jain *et al.*, 2007) and shown in Equation (2.1).

$$\text{Mie theory: } C_{ext} = \frac{24\pi^2 R \epsilon^{3/2} M}{\lambda} \frac{\epsilon_2}{(\epsilon_1 + 2\epsilon_M)^2 + \epsilon_2^2} \quad (2.1)$$

where,  $\epsilon = \epsilon_1(\lambda) + i\epsilon_2(\lambda)$  is the wavelength dependent, complex dielectric function of the nanoparticles materials,  $\epsilon_M$  is the dielectric permittivity of the medium,  $\lambda$  is the incident light wavelength,  $R$  is the particles radius.

According to Equation (2.1),  $C_{\text{ext}}$  is proportional to particle radius hence indicating SPR band intensity increases with the increase in the particle radius. It has been shown that the growth of Ag nanoparticles is accompanied by the increase of SPR absorption band intensity and broadening of SPR band (Mertens *et al.*, 2004). Factors that contribute to the electric oscillations were due to acceleration of the conduction electrons by the electric field, presence of restoring forces, and confinement of the electrons to dimensions smaller than the wavelength of light (Ravindran *et al.*, 2013).

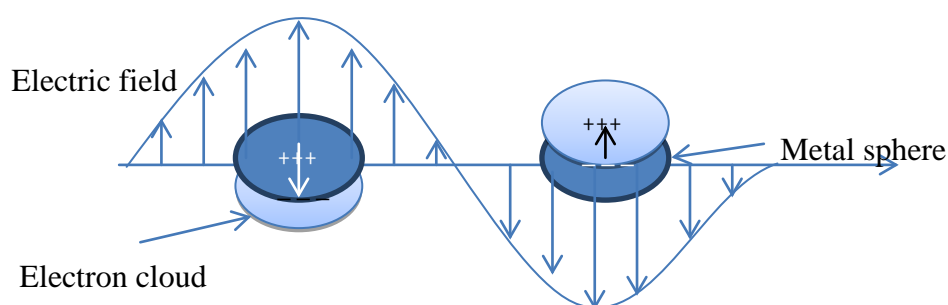


**Figure 2.2** Interaction of electromagnetic radiation with metal nanoparticles  
(Willels and Van Duyne, 2007)

It was reported by Nie and Emory (1997), the size-dependent localized surface plasmon resonance contributes to surface enhanced Raman signals for the detection of single molecules. Hence, the detection of various biomolecules using SERS plasmonic sensors has received significant attention. Shanmukh *et al.* (2008) reported Ag nanorod were used to determine the Raman spectra of Respiratory Syncytical Virus. The extraordinary power of SERS exhibited by Ag nanoparticles as biosensors is being increasingly exploited in nanodiagnostic and nano-imaging industries.

### 2.2.2 Antimicrobial properties of silver nanoparticles

Besides optical properties, Ag possesses powerful antimicrobial properties in its bulk material and is historically recognized as a powerful biocide against bacteria, viruses and fungi. Decreasing particle dimensions into nanosizes have manifested on the physical properties over bulk materials (Chulovskaya and Parfenyuk, 2009). Ag nanoparticles were reported to be highly dispersed and posed higher surface area which indirectly intensified antimicrobial properties and served as an effective antimicrobial agent (Illic *et al.*, 2009). Pal *et al.* (2007) also discovered that besides size, shape of the nanoparticles is also important for antimicrobial activity, with triangular nanoparticles showing higher antibacterial activity compared to other shapes. In addition, Cho *et al.* (2005) reported functionalizing material on Ag nanoparticles was important and could influence the activity with the target microorganism.

Issues in antibiotic resistance in pathogenic and opportunistic microorganisms are dramatically increasing. Although new antibiotics have been constantly developed and introduced to the pharmaceutical industry, none of them were susceptible to the multidrug-resistant bacteria (Conlon *et al.*, 2004). According to Silver and Phung (1996), the antibacterial effects of Ag salts have been noticed since antiquity where Ag nanoparticles have demonstrated strong antimicrobial activities in recent year. Therefore, Ag nanoparticles are considered an attractive alternative to antibiotics. It was also reported that Ag ions and Ag based compounds were highly toxic to microorganisms, thus showing strong biocidal effects to as many as 12 species of bacteria including *Escherichia coli* (Zhao and Stevens, 1998). Aymonier *et al.* (2002) then showed that hybrids of Ag nanoparticles with amphiphilic hyperbranched macromolecules exhibited effective antimicrobial surface

coating agents. Recently, researchers have shown Ag nanoparticles exhibited antiviral and cytotoxic properties against human immunodeficiency virus (HIV), hepatitis B virus (HBV) and H1N1 influenza A virus (Elechiguerra *et al.*, 2005; Xiang *et al.*, 2011; Trefry and Wooley, 2012).

The antimicrobial effects of silver and their derivatives are well documented, however the mechanisms by which it exerted its bioactivity are still unclear. Several proposals have been developed to explain the mechanisms for the bactericidal effects of silver ion/silver metal on bacteria. It was reported that heavy metals reacted with proteins by combining cysteine (CySH) and thiol (-SH) groups such as sodium thioglycollate, which then lead to the inactivation of the proteins (Liau *et al.*, 1997; Lehninger *et al.*, 2011). Also, it was reported that silver in an oxygen-charged aqueous media catalysed the complete destructive oxidation of microorganisms (Davies and Etris, 1997). While various hypotheses have been proposed to explain the mechanism of antimicrobial activity of Ag nanoparticles, it was widely believed that Ag nanoparticles was incorporated in the cell membrane, which caused leakage of intracellular substances and eventually caused cell death (Sondi and Salopek-Sondi, 2004; Cho *et al.*, 2005).

Nevertheless, it was reported that the bactericidal effect of Ag nanoparticles decreased as their size increased, and the shape of their particles is also an important influencing factor for their bactericidal power (Panacek *et al.*, 2006; Pal *et al.*, 2007). Although most studies have utilized spherical particles, Pal *et al.* (2007) showed that truncated triangular shape particles have greater bactericidal effect compared to that of spherical and rod-shaped particles. Concisely, the antimicrobial activity of silver nanoparticles was reported to have comparatively better than the prominent broad-spectrum antibiotics used in the pharmaceutical market (Roy *et al.*, 2007).

The antimicrobial activity of Ag nanoparticles were often determined by using minimum inhibitory concentration (MIC), minimum bactericidal concentration (MBC), half effective concentration ( $EC_{50}$ ), median lethal dose ( $LD_{50}$ ), well-diffusion and disc diffusion methods. Table 2.1 showed the antimicrobial activity of Ag nanoparticles with different sizes and concentrations acting on various pathogens. Although Ag nanoparticles showed strong antimicrobial action towards microorganisms, the exact mechanism of action of Ag nanoparticles on the microbes for its excellent antimicrobial properties is still not known, but the possible mechanisms of action have been suggested according to the morphological and structural changes found in the bacterial cells as illustrated in Plate 2.2.

Feng *et al.* (2000) suggested that silver ions enter into the bacterial cells by penetrating through the cell wall and consequently alter the DNA into a condensed form which reacted with the thiol group proteins and result in cell death. Cho *et al.* (2005) in the research suggested two possibilities of antimicrobial action. The negatively charged surface of the sodium dodecylsulfate interferes with the absorption surface of microbial which has negative charges on the surface of Ag nanoparticles. The other reason suggested for the absorption of Ag was due to the dissolved Ag ions in Ag nanoparticles solution that probably interacted directly with the negatively charged SDS. This electrostatic effect prevents the interaction between Ag ion and microbial system. Ruparelia *et al.* (2008) demonstrated the antimicrobial activity due to the release of ions. The presence of nanoparticles in suspension would ensure continuous release of ions into the nutrient media. Silver ions released by the nanoparticles may attach to the negatively charged bacterial cell wall and cause a rupture, and thereby leading to protein denaturation and cell death. Siva Kumar *et al.* (2004) proposed that oxygen associates with silver and reacts with

the sulfhydryl (-S-H) groups on cell wall to form R-S-S-R bonds thus blocking respiration and cause death of cells. Meanwhile Lok *et al.* (2006) reported that the attachment of both silver ions and Ag nanoparticles to the cell wall may cause accumulation of enveloped protein precursors which resulted in dissipation of the proton motive force. Ag nanoparticles also exhibited destabilization of the outer membrane and rupture of the plasma membrane, thereby causing depletion of intracellular ATP.

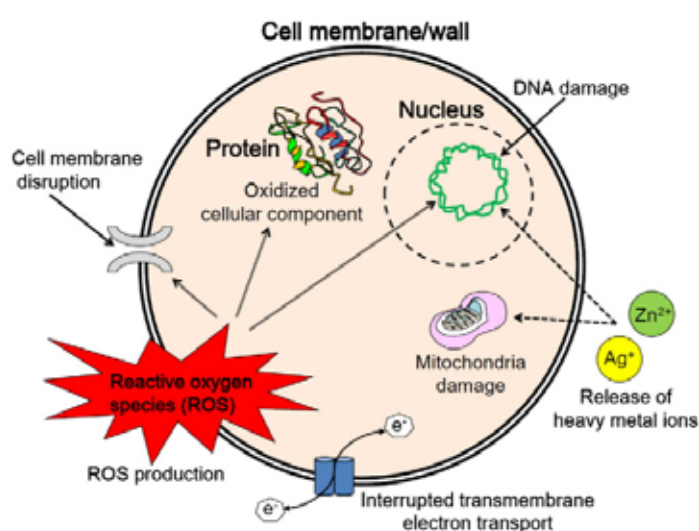


**Plate 2.2** Proposed mechanistic action of Ag nanoparticles on microorganism  
(Huh and Kwon, 2011)

Ag nanoparticles have been shown to be a promising antimicrobial agent and considered as an option for antiviral treatments. It was reported that Ag nanoparticles can inhibit viral replication of viruses such as HIV-1 (Elechiguerra *et al.*, 2005; Lara *et al.*, 2010), hepatitis B virus (Lu *et al.*, 2008), respiratory syncytial virus (Shanmukh *et al.*, 2008; Sun *et al.*, 2008), herpes simplex virus type 1 (Baram-Pinto *et al.*, 2009), monkeypox virus (Rogers *et al.*, 2008), H1N1 influenza A virus (Xiang *et al.*, 2011), avian influenza virus, H5N1 (Jazayeri *et al.*, 2012), etc. Hence, it is



**Table 2.1** Overview of the antimicrobial activity of Ag nanoparticles produced in different sizes

References	Sizes & Concentration	Pathogen	Antimicrobial method	Inhibition
Martinez-Gutierrez <i>et al.</i> (2010)	20 - 25 nm 107.8 µg/mL	<i>B. subtilis</i> , <i>M. bovis</i> , <i>M. smegmatis</i> , <i>MRSA</i> , <i>S. aureus</i> , <i>A. baumannii</i> , <i>E. coli</i> <i>A. niger</i> , <i>C. albicans</i> , <i>C. neoformans</i> THP-1 cells	MIC  LD <sub>50</sub>	0.4 - 1.7 µg/mL  3 - 25 µg/mL 10 ± 3.4 µg/mL
Nanda and Saravanan (2009)	2 µg / 20 µL	<i>MRSA</i> , <i>MRSE</i> , <i>S. pyogens</i> , <i>S. typhi</i>	Well diffusion	11 - 18 mm
Ruparelia <i>et al.</i> (2008)	2.26 - 10.34 nm	<i>E. coli</i> , <i>B. subtilis</i> , <i>S. aureus</i>	MIC MBC	40 - 180 µg/mL 60 - 220 µg/mL
Wani <i>et al.</i> (2013)	8 - 40 nm	<i>E. coli</i>  <i>C. albicans</i>	MIC Disc diffusion MIC Disc diffusion	50 - 100 µg/mL 8 - 16 mm 30 - 60 µg/mL 13 - 24 mm
Bankura <i>et al.</i> (2012)	0.2 mg/mL	<i>B. subtilis</i> , <i>B. cereus</i> , <i>E. coli</i> , <i>S. aureus</i> and <i>P. aeruginosa</i>	Disc diffusion	21 - 36 mm
Logeswari <i>et al.</i> (2013)	22.3 - 65 nm	<i>S. aureus</i> , <i>P. aeruginosa</i> , <i>E. coli</i> and <i>K. pneumoniae</i>	Well diffusion	12 - 30 mm
Sathishkumar <i>et al.</i> (2009)	2 - 50 mg/L	<i>Escherichia coli</i> BL-21	EC <sub>50</sub>	11 ± 1.72 mg/L
Sintubin <i>et al.</i> (2011)	11.2 ± 0.9 nm	<i>S. aureus</i> , <i>E. coli</i> , <i>P. aeruginosa</i>	MBC	50 - 200 mg/L

interesting to study the interaction between Ag nanoparticles and the particular viruses that caused their inactivation. Elechiguerra *et al.* (2005) conducted a high angle annular dark field (HAADF) scanning transmission electron microscopy to study the interaction of Ag nanoparticles with HIV-1 as illustrated in Plate 2.2 It was clearly shown that Ag nanoparticles were bound to the viral shell and caused the inactivation. The viral shell generally comprised of a lipid membrane intermingled with glycoprotein knobs consisting of gp120 surface glycoprotein and gp41 transmembrane glycoprotein connected with protein p 17 (Forster *et al.*, 2000). It was believed that Ag nanoparticles attacked the gp120 surface glycoprotein which plays the key role in recognition and binding of the viral particle to the host cell through the receptor region CD-4.

### **2.3 Market analysis on Ag nanoparticles**

The antibacterial, antifungal and antiviral properties of Ag nanoparticles have been well known. Hence it is necessary to study the market demand of Ag nanoparticles locally and globally to ensure a constant supply to fit consumer needs.

#### **2.3.1 Global market on nanoparticles research**

With the emerging markets of nanotechnology, the 2013 National Federal Budget of United States have provided US\$1.8 billion for the National Nanotechnology Initiative (NNI) in the development of nanotechnology (Nano.org, 2000). According to Bombourg (2012) in the research report titled “Nanotechnology Market Forecast to 2014”, the United States nanotechnology market is rapidly growing with CAGR of about 19% during the year 2011-2014. The most prominent

field in nanotechnology involved mostly the biomedical, biopharmaceutical and electronics industries. Highsmith (2012) stated that the total market values for nanoparticles in biotechnology, drug development and drug delivery have been increased from US\$ 16 billion in 2011 to US\$ 24 billion in 2012 and expected to increase at least 3-fold in year 2017 as illustrated in Figure 2.3.

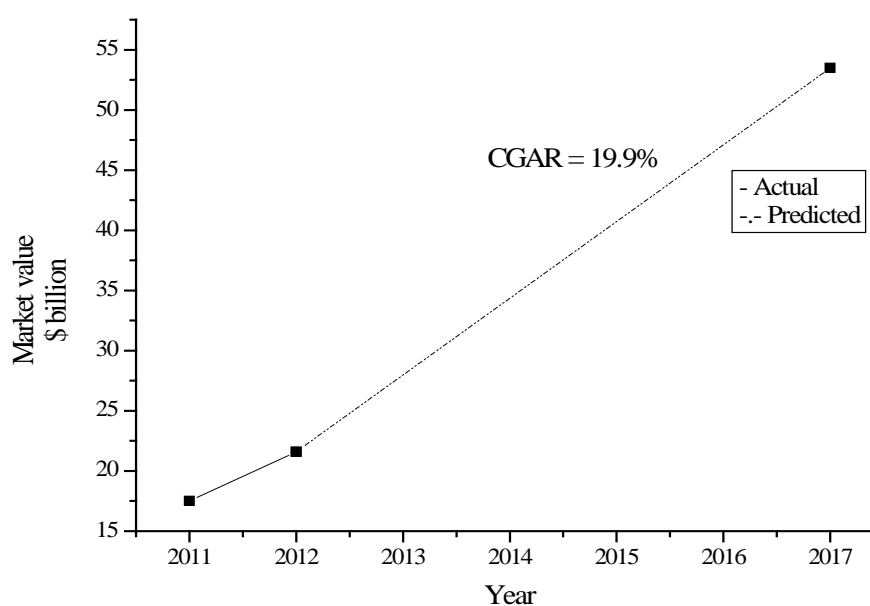


**Figure 2.3** Total market values for nanoparticles in biotechnology, drug development and drug delivery (Source: National Nanotechnology Initiative, <http://www.nano.gov/>)

Of all the nanoparticles, Ag nanoparticles have been reported as the highly developed nanoparticles. As shown in Figure 2.4, Ag nanoparticles associated products have increased about 12-fold in year 2011 from year 2006 according to Rejeski *et al.* (2011).

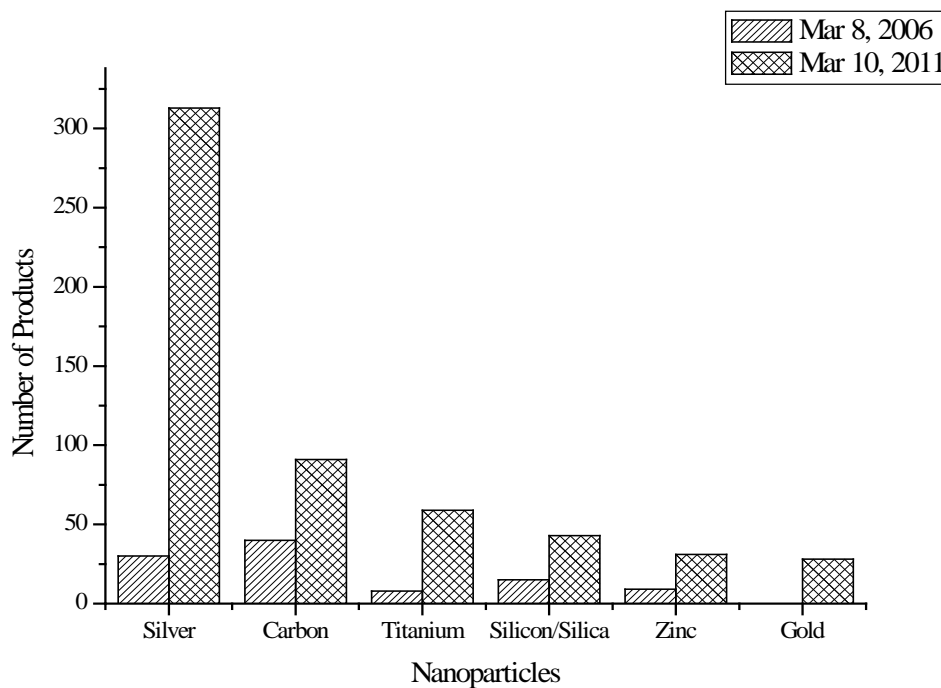


**Figure 2.4** Numbers of products associated with specific nanoparticles (Source: The Project on Emerging Nanotechnologies, [www.nanotechproject.org](http://www.nanotechproject.org))

### 2.3.2 Nanotechnology industries in Malaysia

The development of nanotechnology has influenced the Asia-Pacific region and was reported that this region has experienced the fastest growth with CAGR pegged at around 52% in the forecast period (NanowerkNews, 2009). In Malaysia, the development of nanotechnology has started since early 2001 under the Intensification of Priority Research Area (IRPA) in Eight Malaysian Plan (8MP) which spanned between 2001 to 2005 and was funded by MOSTI (Hashim *et al.*, 2009). They reported that the main research focused on three categories such as material and manufacturing, nanoelectronic and computer technology, and life sciences/ medicine and health. Although in Malaysia, nanotechnology is still at its infancy, the initiative in forming National Nanotechnology Directorate (NND) has showed the pivotal role in coordinating and synergizing the development of